Progress In Electromagnetics Research Letters, Vol. 95, 33–42, 2021

A New Equivalent Circuit Scheme for Grounded Back-to-Back GCPW-MS-GCPW Transitions Fabricated on a Thin Low-k Substrate

Pierre-Vincent Dugue[1, 2, *], Mohammed El-Gibari[1], Mathieu Halbwax[2], Stephane Ginestar[1], Vanessa Avramovic[2], Jean-Pierre Vilcot[2], and Hongwu Li[1]

Abstract—We hereby present a new equivalent circuit model including both lumped and distributed elements for GCPW-MS transitions (GCPW for Grounded Coplanar Waveguide and MS for Microstrip). In order to validate the modelling results, such transitions have been fabricated on a 20 µm-thick BCB (Benzocyclobutene resin) substrate using grounding pads including via-holes of different diameters. The study focused on the impact of the via-hole diameter on the performance of the transition and more specifically on its bandwidth. The transitions were made using a simple technological process based on photosensitive polymer. ADS simulation data of the new equivalent circuit model were in very good agreement with measured S-parameters. Both theoretical and experimental results have shown that the bandwidth of such a transition can reach up to 100 GHz using via-holes of 900 µm diameter.

1. INTRODUCTION

The evolution in the mobile communications that we have witnessed for 20 years raises a lot of interest in radio frequency (RF) systems. Connected devices and civil/military communications are certainly sectors targeting the increase in the working frequency range [1]. The amount of requests for devices allowing users to get seamless high data-rate signals processing is increasing day by day. Notably, Monolithic Microwave Integrated Circuits (MMICs) focus interest in reducing their footprint and increasing their operation bandwidth by adjusting the embedded transmission lines and transitions. Bandwidth optimization of many transitions has already been explored on thick film substrates [2–4]. It results in the integration of multiple via-holes along the transitions to reduce losses and improve mode conversion.

Hereby, we seek to validate a new equivalent circuit model over an ultra-large bandwidth and to demonstrate the feasibility of a microwave transition between a Grounded Coplanar Waveguide (GCPW) line and a Microstrip (MS) line in a thin film configuration as encountered in MMICs. The single via solution that is used for the grounding pads of the GCPW portion is optimized, and the bandwidth is increased up to 110 GHz. Furthermore, this transition design could be a great solution in domains like multiple layers MMICs which need high integration level and in new domains such as microwave photonic devices [5, 6].

Received 30 September 2020, Accepted 24 November 2020, Scheduled 9 December 2020

* Corresponding author: Pierre-Vincent Dugue (pierre-vincent.dugue@etu.univ-nantes.fr).
[1] Université de Nantes, CNRS, Institut d'Électronique et des Technologies du numéRique (IETR UMR 6164), UFR des Sciences et des Techniques, 2 Chemin de la Houssinière, 44322 Nantes cedex, France.
[2] Univ. Lille, CNRS, Centrale Lille, Yncréa ISEN, Univ. Polytechnique Hauts-de-France, UMR 8520-IEMN, F-59000 Lille, France.

2. METHODS

2.1. HFSS Modelling

In order to discern the impact of single via-hole grounding pads on the performance of a GCPW-MS transition, such a structure has been modelled using High Frequency Structure Simulator (HFSS) software. A back to back GCPW-MS-GCPW component has been modelled since it corresponds to the practical case that will be used for characterization. The layout of the component is shown in Figure 1. The overall length of the transition is $L = 1\,\text{cm}$. The grounding pad dimensions are: width $S = 1\,\text{mm}$ and length $L1 = 1\,\text{mm}$. The gap between the pad and center line is 25 µm. The MS line is 54 µm wide. The substrate thickness is 20 µm. The bottom (T_{ground}) and top metallization (T_{ms}) thicknesses are 200 nm and 900 nm, respectively. More details on materials can be found in Section 2.2 which is relative to the component fabrication. The diameter (D) of the via-holes varies from 100 to 900 µm.

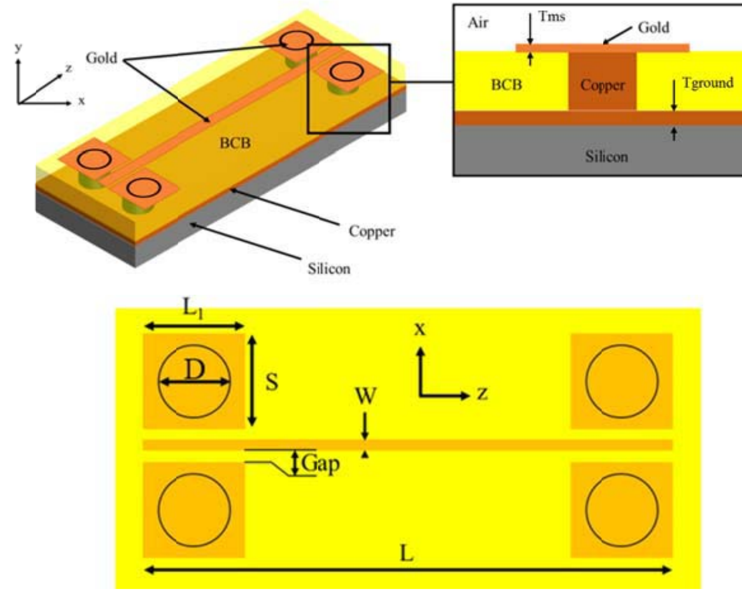

Figure 1. Modelled GCPW-MS-GCPW transition including input and output coplanar-microstrip transitions with grounding via-holes and a microstrip transmission line in between.

The results of HFSS simulation are given in Figures 2(a) and 2(b). Cutoff frequency is determined by either an S_{21} value at $-3\,\text{dB}$ from its value in the low frequency range ($-0.5\,\text{dB}$ @ 250 MHz here), so at $-3.5\,\text{dB}$ or an S_{11} value below $-10\,\text{dB}$. Apart from the inherent propagation losses of the MS line, the resonance peaks of the S_{21} curves, due to the parasitic inductance of the via-holes, are the main factor of bandwidth reduction, as shown by Goldfarb and Pucel [6]. The parasitic inductance L_{para} of a metallized cylindrical via-hole is directly related to its volume and can be expressed as follows:

$$L_{para} = \frac{\mu_0}{2\pi} \cdot \left[h \cdot \ln \left(\frac{h + \sqrt{r^2 + h^2}}{r} \right) + \frac{3}{2} \left(r - \sqrt{r^2 + h^2} \right) \right] \tag{1}$$

where μ_0 is the vacuum permeability; h is the depth of the via-hole, equal here to the substrate thickness T_{BCB}; and r is its radius. According to this expression that is valid for dielectric thickness values less than 3% of the free-space wavelength of the working frequency, the via-hole inductance increases when its depth increases, and its radius diminishes. This directly supports the fact that bandwidth limitation is reduced using thin substrates and large via-hole diameters. For example, for $T_{sub} = 635\,\mu\text{m}$, $L_{para} = 0.23\,\text{nH}$ and 0.47 pH respectively for via-hole diameters of 100 µm and 900 µm. Those values are respectively 405 fH and 44.5 fH when a substrate thickness $T_{sub} = 20\,\mu\text{m}$ is used.

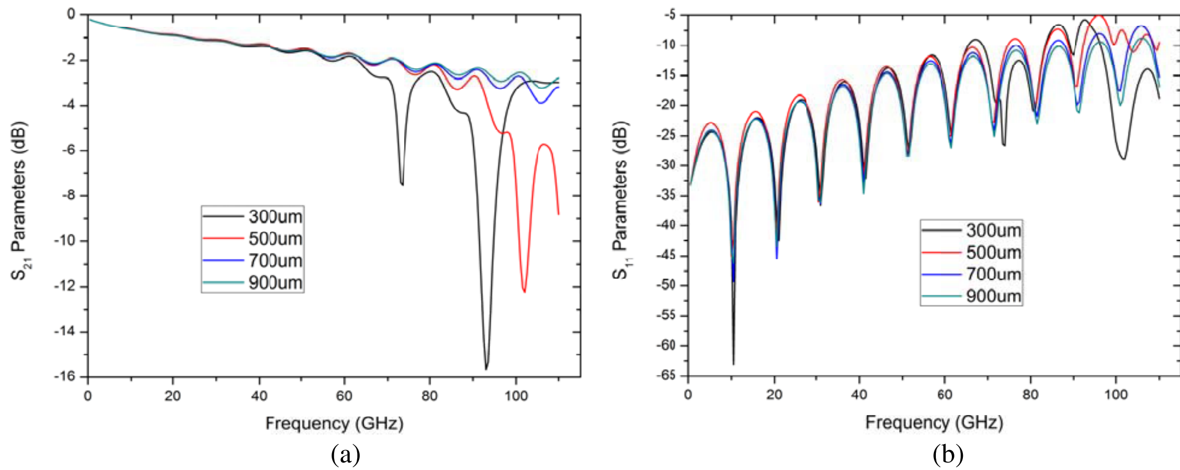

Figure 2. Simulated S-parameters issued from HFSS modelling as a function of the via-hole diameter: (a) S_{21} and (b) S_{11}.

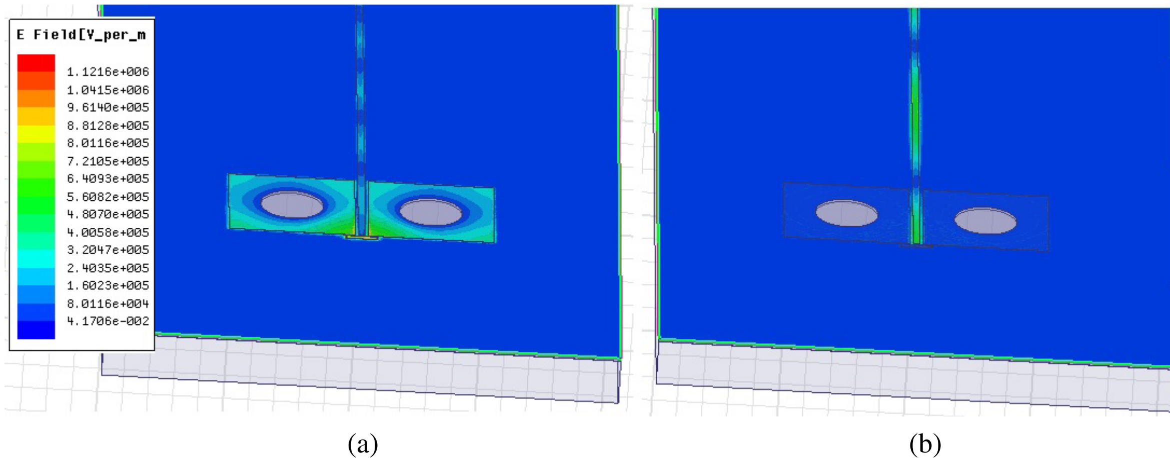

Figure 3. Electric field distributions for a GCPW-MS transition obtained by HFSS simulation at (a) resonant frequency (102.5 GHz) and (b) operating frequency (40 GHz).

When via-hole diameter is increased, the S_{21} resonance peaks tend to be pushed towards higher frequency range, allowing a bandwidth around 100 GHz to be reached for via-hole radius of 900 μm. The deduced bandwidths are summarized in Table 1 versus the via-hole diameter.

Figure 3 shows the electric field distributions obtained by HFSS simulation for a transition, using 500 μm-diameter via-holes, for two representative frequencies, one corresponding to the major resonant peak at 102.5 GHz (Figure 3(a)) and the other in the transmission band, i.e., outside the resonant peak, here at 40 GHz (Figure 3(b)). It is noticeably observed that, at resonance frequency, the main part of the electric field is concentrated on the ground pads and that little energy is then propagating on the MS line whereas it is completely the reverse situation in the operating bandwidth of the transition.

2.2. Fabrication of the GCPW-MS-GCPW Component

The component has been fabricated following the layout shown in Figure 1. The substrate material is BCB (Benzocyclobutene resin). The metallic layer of the bottom ground plane and the via-hole filling are made of copper. The top metallization is made of gold that has been chosen mainly owing to its compatibility with the microwave probing equipment. The mask layout incorporates all the component

Table 1. HFSS simulation of GCPW-MS-GCPW component as function of the via-hole diameter: the cutoff frequency is defined by the lowest of the two values corresponding to: $S_{21\,\mathrm{dB}} \geq -3.5\,\mathrm{dB}$ or $S_{11\,\mathrm{dB}} \leq -10\,\mathrm{dB}$.

Via-hole diameter (μm)	$S_{21\,\mathrm{dB}} \geq -3.5\,\mathrm{dB}$ (GHz)	$S_{11\,\mathrm{dB}} \leq -10\,\mathrm{dB}$ (GHz)	Cutoff frequency (GHz)
100	47.3	47.3	47.3
200	58.8	56.6	56.6
300	70.7	65.5	65.5
400	76.9	74.6	74.6
500	84.4	74.7	74.7
600	85.9	75.5	75.5
700	94.3	76.4	76.4
800	95.4	85.5	85.5
900	104.1	95.1	95.1

variants mentioned above, i.e., components with via-hole diameters from 100 μm up to 900 μm by 100 μm step. This allows a collective fabrication of all components ensuring the different material layers to be identical from one component to another, removing some possible error sources comparing experimental results between variants.

2.2.1. Processing Flow

The substrate is made of a photosensitive BCB: Cyclotene™ XUS35078-Type 3 from Dow® [7]. Its permittivity, ε_r, is 2.65, and it has been particularly chosen for its low value of dielectric loss tangent ($\tan\delta = 0.0008$ @ 20 GHz), for the thicknesses that can be deposited (a wide range from 15 μm to 40 μm for the formulation used) and for the advantages brought by its photosensitive nature. Indeed in a lot of devices, via-holes are opened using etching techniques like RIE (Reactive Ion Etching), DRIE (Deep Reactive Ion Etching), ICP (Inductively Coupled Plasma) [8–10], or inkjet printing [11] in the substrate (polymer, metal, silicon), which makes the manufacturing process complicated and expensive. For this demonstration purpose, using photosensitive BCB is simple because it allows opening the via-holes just using a lithography process.

The process is presented below (Figure 4).

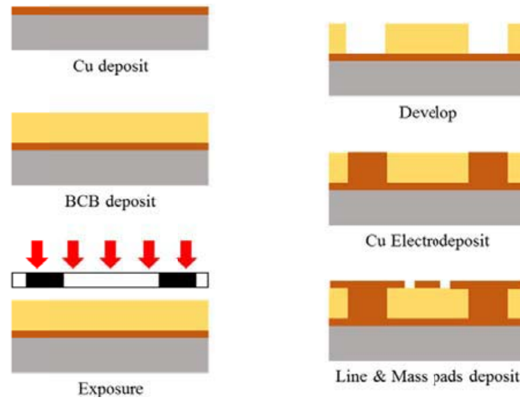

Figure 4. Process flow (main steps) for the component fabrication.

Main fabrication steps are:

- metallization of the bottom ground plane (200 nm) by sputtering deposition of a Ti/Cu layer (Ti is used as adhesion layer);
- deposition of BCB (around 20 µm) by spin-coating;
- lithography of BCB defining via-hole;
- via-hole filling by electrodeposition of copper;
- lithography of top layer metallization;
- metallization of top ground pads and MS line (400 nm) by e-beam evaporation of Ti/Au layer (Ti is used as adhesion layer);

2.2.2. Substrate Deposition

The components are fabricated on a 3″ silicon wafer. Before dielectric film is deposited, the bottom ground plane is full-wafer deposited using the sputtering deposition of, firstly, a layer of 20 nm-thick titanium that plays the role of adhesion layer and, secondly, a layer of 300 nm of copper. Then, a 27 µm-thick BCB XUS35078 film is deposited by spin-coating (a primary spin coat of adhesion promoter AP3000 was made). This allows to get a final thickness about 20 µm (DOW® recommends to have 6–7 µm thicker film than the desired value at spin-coat level since the post-bake process tends to densify the material and to reduce its thickness). A soft bake at 110°C was made on a hot plate prior to exposure in order to remove any residual solvent.

2.2.3. Opening of the Via-Holes

The exposure of the via-hole patterns has been performed on a MA6/BA6 Suss MicroTec UV240-UV 400 nm at 500 mJ/cm^2 for 200 s. Development was made by immersion in DS3000 developer @ 35°C for 7 minutes; it allows a total opening of via-hole patterns (Figure 5(a)). A profilometer measurement shows complete opening of the via-holes just after development (Figure 5(b)). A post-bake at 250°C for 30 minutes was then performed to totally harden the BCB material.

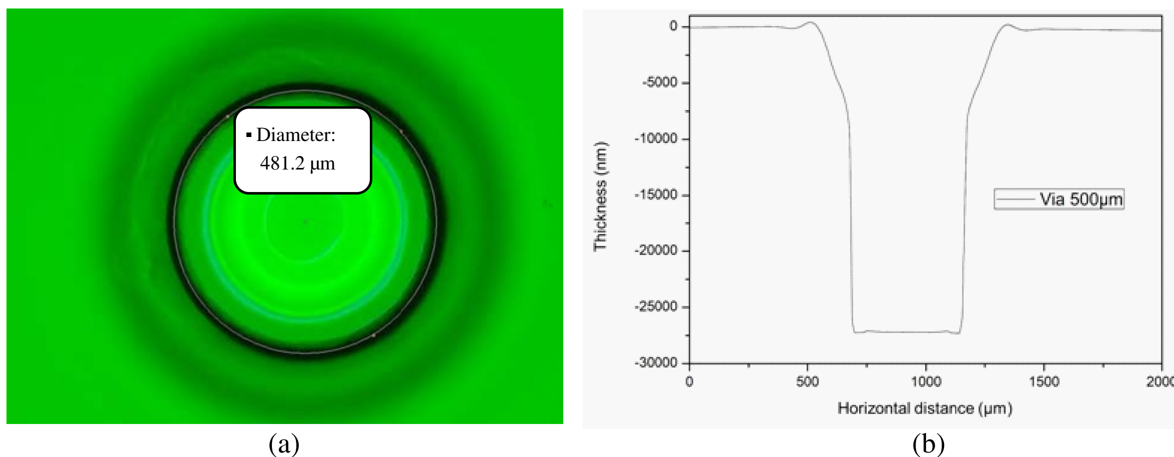

Figure 5. (a) Optical microscope view of a 500 µm-diameter via-hole pattern under development; (b) Corresponding profilometer measurement prior to the BCB post-bake.

2.2.4. Via-Holes Filling by Electrodeposition

Copper electrodeposition process has been widely used for via-hole filling [12, 13]. Patterned BCB sample was dipped jointly with a copper bar inside an electrolytic bath of sulfuric acid and water. The bath is agitated at 200 rpm to maintain a uniform electrolytic behavior by keeping a homogeneous volume concentration of molecules. A voltage of 0.1 V and a current of 4.1 µA are applied on the sample for 7 minutes to achieve the full via filling.

2.2.5. Deposition of the GCPW-MS-GCPW Electrode Structure

Lithography of the top level has been made using AZ1512HS photoresist from Clariant® because it offers a good undercut profile, an essential condition for the next lift-off process. A 20 nm-thick Ti layer and a 900 nm-thick Au layer were then full-wafer deposited. E-beam evaporation was used in order to ease the lift-off process. The latter was made using AR 300-76 stripper (Allresist) @ 75°C for 60 minutes. The AR 300-76 stripper was chosen since it has no effect on the BCB layer contrary to other possible stripper solutions. The result, after lift-off, is shown in Figure 6.

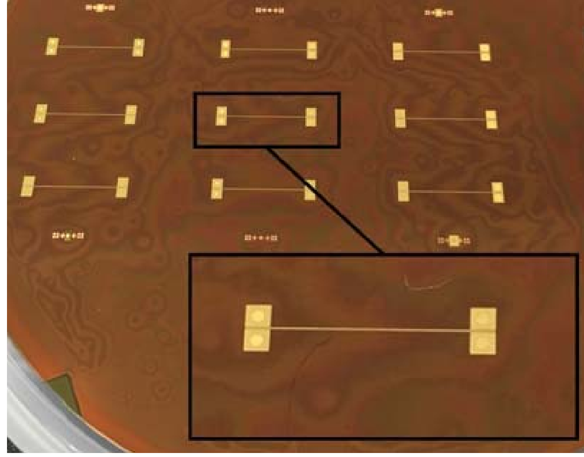

Figure 6. Part view of the wafer on which a set of nine components, each of them including transitions with different via-hole diameters, from 100 μm to 900 μm, has been fabricated.

3. EXPERIMENTAL RESULTS

The characterization has been carried out with a vector network analyzer (VNA) R&S® ZVA 24 associated with ZVA-Z110 heads and GSG 100 Infinity^{TM} probes allowing the measurement of S-parameters over the frequency range from 250 MHz to 110 GHz. An LRRM (Line-Reflect-Reflect-Match) calibration method is performed preliminarily using a Cascade ISS-104-783 calibration substrate. The system is controlled by Wincal Cascade software. Measured results (Figure 7 and Table 2) are in good agreement with those obtained with HFSS electromagnetic simulation (cf. Figure 2). Resonant peaks appear at the same frequency, and the response is damped, as usual, compared to that obtained in simulation. For via-hole diameter above 700 μm, no resonant peak is observed in the measurement frequency band, and the transition bandwidth is superior to 110 GHz.

4. EQUIVALENT CIRCUIT MODELLING

Wiatr et al. proposed an equivalent circuit for such a GCPW-MS transition (only one via-hole centered in the top ground pad) fabricated on a thick (175 μm) and high permittivity (10) substrate [14]. The proposed circuit was validated over a 30 GHz bandwidth; we used it as a basis and adapted it to extend its validity to thin and low permittivity substrates as well as to a larger bandwidth, 100 GHz typically. The new equivalent circuit (Figure 8) differs by a residual capacitance C_{Via} that appears between the superior ground pad of the via-hole and the bottom ground plane and by a resistance R_{Via} related to the via-hole metallization. The GCPW-MS transition is now modelled by:

- C_{Via}, R_{Via}, and L_{Via} which are the three elementary components representing the via-hole,
- C_{coupl} and L_{coupl} are respectively the coupling capacitance and the link inductance between ground pads and microstrip line, and R_{coupl} is the resistance related to L_{coupl}.

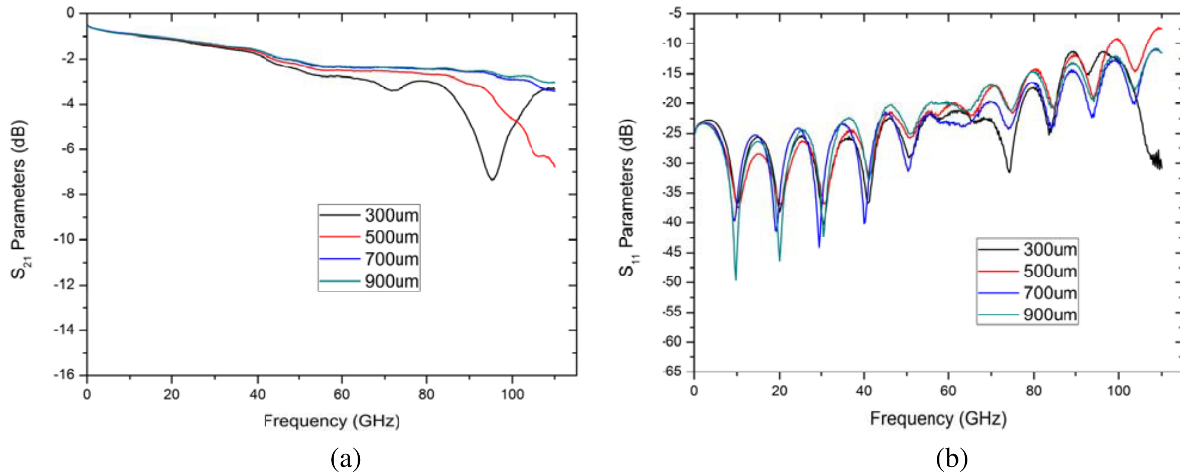

(a) (b)

Figure 7. Measured S-parameter as function of the via-hole diameter: (a) S_{21} and (b) S_{11}.

Table 2. Measurement of the S-parameters of GCPW-MS-GCPW components as function of the via-hole diameter: the cutoff frequency is defined by the lowest of the two values corresponding to $S_{21\,\mathrm{dB}} \geq -3.5\,\mathrm{dB}$ and $S_{11\,\mathrm{dB}} \leq -10\,\mathrm{dB}$.

Via-hole diameter (μm)	$S_{21\,\mathrm{dB}} \geq -3.5\,\mathrm{dB}$ (GHz)	$S_{11\,\mathrm{dB}} \leq -10\,\mathrm{dB}$ (GHz)	Cutoff Frequency
100	46.5	over 110	46.5
200	82.25	88.0	82.25
300	85.75	over 110	85.75
400	84.5	97.0	84.5
500	94.75	98.0	94.75
600	95.25	97.25	95.25
700	over 110	over 110	over 110
800	over 110	over 110	over 110
900	over 110	over 110	over 110

The microstrip section between the two GCPW-MS transitions is represented by a distributed element available in the ADS library, which allows ADS simulation to be easy, accurate, and fast.

Each passive element value has been optimized (Table 3) to fit the ADS simulated and experimental S-parameters values within 10% difference.

Table 3. Component values extracted from ADS after optimization.

Via-hole diameter	300 μm	500 μm	700 μm	900 μm
C_{via}	6.04 fF	6.17 fF	6.12 fF	6.51 fF
L_{via}	950 pH	765 pH	546 pH	352 pH
R_{via}	408 Ω	388 Ω	406 Ω	401 Ω
C_{coupl}	10.8 fF	10.5 fF	8.00 fF	13.1 fF
L_{coupl}	977 pH	643 pH	598 pH	356 pH
R_{coupl}	1.02 Ω	53.9 Ω	191 Ω	287 Ω

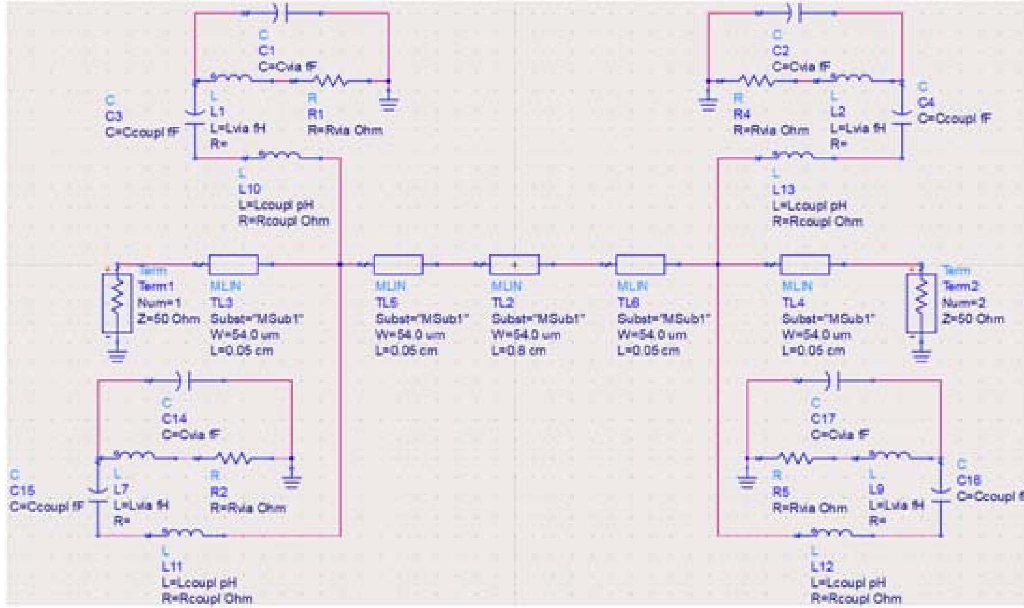

Figure 8. Equivalent circuit of the GCPW-MS-GCPW component shown in Figure 1. Lumped and distributed elements are used to model the vias and the MS line, respectively.

First, the via-hole capacitance, C_{via}, remains the same whatever the diameter is; the intrinsic capacity related to the via-hole is slightly affected due to the low variation in the dimensions of the ground pad, especially. L_{via} logically decreases with the increase in via-hole diameter, roughly by 200 pH every 200 µm. R_{via} remains unchanged, around 400 Ω. The value of C_{coupl}, the capacitance which appears between the ground pad and the microstrip line, does not change significantly, around 10 fF whatever the diameter is; in fact, the gap between the ground pad and the MS line does not change either, explaining this invariance. L_{coupl} also tends to decrease, same as L_{via}, following pretty much the same tendency. Finally, R_{coupl} shows an increase with diameter increase; this is almost unexplained right now, a behavior like that observed for C_{coupl} would have been awaited.

The comparison between the simulation results obtained using this equivalent circuit on ADS and the measured S-parameters values shows a good agreement on their overall behavior and, especially, on the position of the resonance peaks (Figure 9). In addition, this equivalent circuit predicts bandwidth values closer to the experimental ones than HFSS simulation does. For example, for a via-hole diameter of 700 µm, due to its overestimation of S_{11} module, HFSS simulation predicts a reflection-limited bandwidth of 76.4 GHz while it is over 110 GHz according to both measurement and ADS simulation results (Figure 9).

There are of course some minor differences between measurement and ADS simulation results concerning:

- the bandwidth limitation for smaller via-hole diameters, e.g., for via-hole diameter of 300 and 500 µm: the values obtained are 81 GHz and 92 GHz, respectively, by ADS modelling versus 85.75 GHz and 94.75 GHz for experimental ones (cf. S_{21} curves on left top graph in Figure 9).
- the discrepancy in reflection coefficient: it is more pronounced for larger via-holes diameters (cf. S_{11} curves on right bottom graph in Figure 9), but fortunately, reflection coefficients for via-hole diameters of 700 µm and 900 µm always remain below the −10 dB criterion. There is so no consequence on bandwidth value.

The supplementary low amplitude oscillations observed on the experimental S_{21} curves can be explained by the experimental positioning of the probes that always leaves a "dead end", i.e., the probes are never positioned at the perfect beginning of the component, resulting in a small echo on the transmission and reflection parameters.

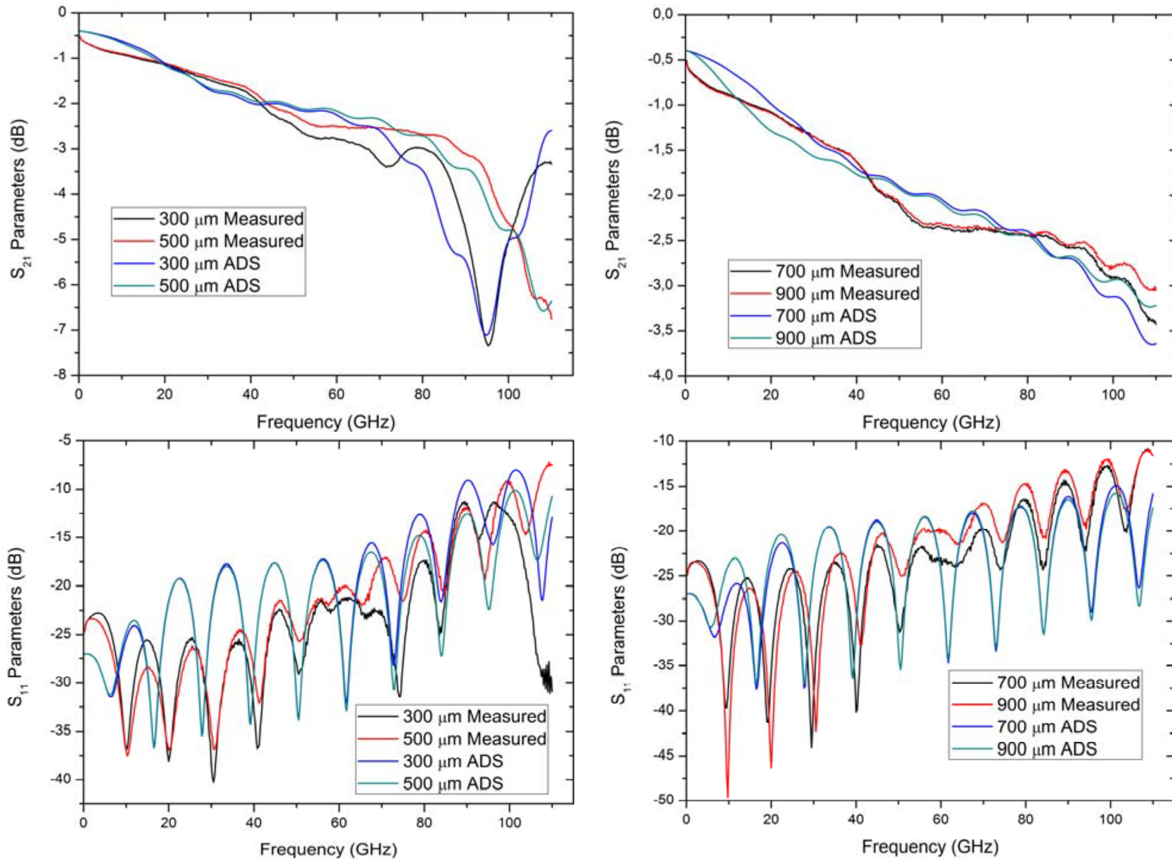

Figure 9. Comparison between ADS simulation and measurement results of the S-parameters of the GCPW-MS-GCPW component shown in Figure 1.

5. CONCLUSION

We studied the influence of the via-hole diameter on the transmission and reflection parameters of a GCPW-MS transition on thin substrate. According to simulation results from HFSS, the bandwidth of such transitions using grounding pads with a single circular via-hole can exceed 100 GHz. GCPW-MS-GCPW components have been fabricated on a 20 μm-thick BCB substrate and measured over the 250 MHz–110 GHz frequency range; the results show a wider bandwidth than the one predicted by HFSS. Based on the equivalent circuit of the GCPW-MS transition proposed by Wiatr et al., an improved model has been developed to reproduce the experimental measurements up to 110 GHz on low permittivity and thin substrates. ADS simulation results using this equivalent circuit showed good agreement with experimental ones. Even if right now, a parametric model has not be fully set, the optimized value of each element constituting this equivalent circuit gives the trend. For the larger fabricated via-hole diameters, i.e., 700 μm and 900 μm, a bandwidth higher than 110 GHz has been recorded, bringing such a GCPW-MS transition on a thin film of BCB as one exhibiting the largest bandwidth currently reported in the literature.

ACKNOWLEDGMENT

The authors would like to thank the support of the French National Research Agency (ANR) and the Directorate General of Armaments (DGA) of the French Armed Forces Ministry under the ADC-Poly project (ANR-17-ASTR-0004). Pierre-Vincent DUGUE got a doctoral fellowship from both DGA (agreement N° 2017 60 0052) and Région des Pays de la Loire (agreement N° 2017-08522). Authors also thank the RENATECH network for its support in device fabrication.

REFERENCES

1. Larson, L., "RF and microwave hardware challenges for future radio spectrum access," *Proc. IEEE*, Vol. 102, No. 3, 321–333, Mar. 2014.
2. Sain, A. and K. L. Melde, "Impact of Ground via placement in grounded coplanar waveguide interconnects," *IEEE Trans. Compon. Packag. Manuf. Technol.*, Vol. 6, No. 1, 136–144, Jan. 2016.
3. Xu, J., C. Sun, B. Xiong, and Y. Luo, "Resonance suppression of grounded coplanar waveguide in submount for 40 Gb/s optoelectronic modules," *J. Infrared Millim. Terahertz Waves*, Vol. 30, No. 2, 103–108, Feb. 2009.
4. Zhou, Z. and K. L. Melde, "Development of a broadband coplanar waveguide-to-microstrip transition with vias," *IEEE Trans. Adv. Packag.*, Vol. 31, No. 4, 861–872, Nov. 2008.
5. Lee, M., H. E. Katz, C. Erben, D. M. Gill, P. Gopalan, J. D. Heber, and D. J. McGee, "Broadband modulation of light by using an electro-optic polymer," *Science*, Vol. 298, 1401–1403, Dec. 2002.
6. Goldfarb, M. E. and R. A. Pucel, "Modeling via hole grounds in microstrip," *IEEE Microw. Guid. Wave Lett.*, Vol. 1, No. 6, 135–137, Jun. 1991.
7. "CYCLOTENE 4000 series — Kayaku advanced materials," Kayaku Advanced Materials, Inc., https://kayakuam.com/products/cyclotene-4000-series/.
8. Kondo, K., U. Suzuki, T. Saito, N. Okamoto, and M. Marunaka, "High-aspect ratio copper-via filling for three dimensional chip stacking," *59th Electronic Components and Technology Conference*, 658–662, San Diego, CA, USA, May 26–29, 2009.
9. Lin, C.-L., P.-S. Chen, Y.-C. Lin, B.-Y. Tsui, and M.-C. Chen, "Via-filling capability of copper film by CVD," *J. Electrochem. Soc.*, Vol. 150, No. 7, C451, May 2003.
10. Wu, B., A. Kumar, and S. Pamarthy, "High aspect ratio silicon etch: A review," *J. Appl. Phys.*, Vol. 108, No. 5, 051101, Sept. 2010.
11. McKerricher, G., J. G. Perez, and A. Shamim, "Fully inkjet printed RF inductors and capacitors using polymer dielectric and silver conductive ink with through vias," *IEEE Trans. Electron Devices*, Vol. 62, No. 3, 1002–1009, Mar. 2015.
12. Josell, D., B. Baker, C. Witt, D. Wheeler, and T. P. Moffat, "Via filling by electrodeposition: Superconformal silver and copper and conformal nickel," *J. Electrochem. Soc.*, Vol. 149, No. 12, C637, Oct. 2002.
13. Lühn, O., C. A. Van Hoof, W. Ruythooren, and J.-P. Celis, "Filling of microvia with an aspect ratio of 5 by copper electrodeposition," *Electrochimica Acta*, Vol. 54, No. 9, 2504–2508, Mar. 2009.
14. Wiatr, W., D. K. Walker, and D. F. Williams, "Coplanar-waveguide-to-microstrip transition model," *2000 IEEE MTT-S International Microwave Symposium Digest (Cat. No. 00CH37017)*, Vol. 3, 1797–1800, 2000.